

Identifying the Higgs boson in electron-photon collisions

O. J. P. Éboli and M. C. Gonzalez-Garcia*
*Instituto de Física, Universidade de São Paulo,
 Caixa Postal 20516, CEP 01498-970 São Paulo, Brazil*

S. F. Novaes
*Instituto de Física Teórica, Universidade Estadual Paulista,
 Rua Pamplona 145, CEP 01405-900, São Paulo, Brazil*
 (Received 7 July 1993)

We analyze the production and detection of the Higgs boson in the next generation of linear e^+e^- colliders operating in the $e\gamma$ mode. In particular, we study the production mechanism $e+\gamma \rightarrow e\gamma\gamma \rightarrow e+H$, where one photon is generated via the laser backscattering mechanism, while the other is radiated via the usual bremsstrahlung process. We show that this is the most important mechanism for Higgs boson production in a 500 GeV $e\gamma$ collider for $M_H \gtrsim 140$ GeV. We also study the signals and backgrounds for detection of the Higgs boson in the different decay channels $b\bar{b}$, W^+W^- , and ZZ , and suggest kinematical cuts to improve the signature of an intermediate-mass Higgs boson.

PACS number(s): 14.80.Bn, 13.10.+q, 42.62.Hk

The most crucial missing element of the standard model is the Higgs boson. Its couplings with all other particles are predicted by the model and once measured can shed some light on the spontaneous symmetry breakdown mechanism. In particular, the one-loop $H\gamma\gamma$ coupling receives contributions from all charged particles that acquire their masses from the Higgs mechanism, and the study of this coupling can provide us with fundamental information about the particle mass spectrum. In this work we analyze the capability of an $e\gamma$ collider to produce and study the Higgs boson properties, in particular its coupling to photons.

An important feature of the next generation of linear e^+e^- colliders (NLC) is that they should also be able to operate in the $e\gamma$ or $\gamma\gamma$ modes. The conversion of electrons into photons can occur via the laser backscattering mechanism [1]. In this case the energy and luminosity of the photon beam would reach almost the same values of the parent electron beam. This makes the NLC a very versatile machine which will be able to use energetic electrons and/or photons as initial states.

In the NLC operating in the e^+e^- mode the most promising mechanisms to produce the standard model Higgs bosons are the Bjorken process, $e^+ + e^- \rightarrow Z \rightarrow Z+H$, and the vector boson fusion mechanism, $e^+ + e^- \rightarrow W^+W^- \rightarrow \nu + \bar{\nu} + H$ [2], where the Higgs boson coupling with W 's and Z 's could be very well determined. However, it is virtually impossible to study the coupling of the Higgs bosons to $\gamma\gamma$ pairs due to the small branching ratio of Higgs bosons into a photon pair. Higher-order electroweak processes for the Higgs boson production, such as $e^+ + e^- \rightarrow VVH$ ($V = W, Z$) [3], could in principle give more information on the Higgs boson couplings, but

unfortunately their total cross sections are rather small.

The standard model Higgs boson can also be produced at the NLC operating in the $\gamma\gamma$ mode, as suggested in Ref. [4]. This mode is particularly interesting since in principle it allows a detailed study of the coupling $H\gamma\gamma$. However, as was pointed out in Ref. [5], resolved photon processes can impose a severe drawback for the Higgs boson detection in the $b\bar{b}$ channel. Another possibility of Higgs boson production is the associated production with the top quark through the process $\gamma\gamma \rightarrow t\bar{t}H$ [6], which is suited for the analyses of the $t\bar{t}H$ coupling. However, for a 500 GeV collider the total cross section for this process is below 0.5 fb for $M_H > 60$ GeV.

In this paper we concentrate on the possibility of identifying the Higgs boson with the NLC operating in the $e\gamma$ mode. We stress that this setup provides us with a rich source of $\gamma\gamma$ interactions when the hard backscattered photon interacts with photons radiated by the electrons in the other beam. This way the Higgs boson can be produced in the process

$$e + \gamma \rightarrow e\gamma\gamma \rightarrow e + H \quad (1)$$

which takes place via the $H\gamma\gamma$ coupling. We show that for a 500 GeV collider, this is the most important mechanism for the production of a Higgs boson with $M_H > 140$ GeV even when compared with the previously suggested [7, 8] associated production $\gamma + e \rightarrow W + \nu_e + H$. We study the $b\bar{b}$, W^+W^- , and ZZ signatures of the Higgs boson and compare it with the possible backgrounds coming from direct and resolved photon processes, and from double vector boson production in $e\gamma$ collisions. We show how convenient kinematical cuts are able to improve in a significant way the signal over background ratio for the intermediate mass Higgs that decays mainly through the heavy quark channel.

The scattering of an energetic electron by a soft photon from a laser allows the transformation of an electron beam into a photon beam whose spectrum is [9]

*Permanent address: Physics Department, University of Wisconsin, Madison, WI 53706.

$$F_L(x) \equiv \frac{1}{\sigma_c} \frac{d\sigma_c}{dx} = \frac{1}{D(\xi)} \left[1 - x + \frac{1}{1-x} - \frac{4x}{\xi(1-x)} + \frac{4x^2}{\xi^2(1-x)^2} \right], \quad (2)$$

with

$$D(\xi) = \left(1 - \frac{4}{\xi} - \frac{8}{\xi^2} \right) \ln(1 + \xi) + \frac{1}{2} + \frac{8}{\xi} - \frac{1}{2(1 + \xi)^2},$$

where σ_c is the Compton cross section, and $\xi \simeq 4E\omega_0/m^2$, with m and E being the electron mass and energy. In our calculation we have chosen the laser energy, ω_0 , in order to maximize the backscattered photon energy without spoiling the luminosity through e^+e^- pair creation by the interaction between the laser and the backscattered photon. This can be accomplished by taking $\xi = 2(1 + \sqrt{2}) \simeq 4.8$. With this choice, the photon

spectrum exhibits a peak close to its maximum which occurs at $x_{\max} = \xi/(1 + \xi) \simeq 0.83$.

Another source of photons is bremsstrahlung from the electrons in the other beam. The spectrum of bremsstrahlung photons can be described by the usual Weizsäcker-Williams distribution

$$F_{\text{WW}}(x) = \frac{\alpha}{2\pi} \frac{1 + (1-x)^2}{x} \ln \left(\frac{E^2}{m_e^2} \right). \quad (3)$$

In the narrow width approximation, the cross section for the process in Eq. (1) can be expressed in terms of the two photon distributions and the width $\Gamma(H \rightarrow \gamma\gamma)$ as

$$\sigma(e + \gamma \rightarrow e\gamma\gamma \rightarrow e + H) = \frac{8\pi^2}{s} \frac{\Gamma(H \rightarrow \gamma\gamma)}{M_H} \int_{\tau_H/x_{\max}}^{x_{\max}} \frac{dx}{x} F_L(x) F_{\text{WW}}(\tau_H/x), \quad (4)$$

where $\tau_H = M_H^2/s$ and \sqrt{s} is the center-of-mass energy of the original e^+e^- collider. Since we are assuming that all of the electron beam is converted into photons and we have performed the convolution with the photon distributions, the corresponding number of events will be given by $N_{\text{ev}} = \mathcal{L}_{e^+e^-} \sigma$, with $\mathcal{L}_{e^+e^-}$ being the luminosity of the e^+e^- machine. The above expression for the cross section is valid for unpolarized photons. If both the laser backscattered photon and the electron are polarized and the radiated photon carries part of the electron polarization, Eq. (4) should be multiplied by a factor $(1 + \langle \lambda_L \lambda_{\text{WW}} \rangle)$, where $\lambda_{L,\text{WW}}$ are the helicities of the corresponding photons.

In Fig. 1(a) we plot the cross section $\sigma(e + \gamma \rightarrow e\gamma\gamma \rightarrow e + H)$ as a function of the Higgs mass for $\sqrt{s} = 500$ GeV for two different top quark masses. For sake of comparison, we also show the cross section for the process $e + \gamma \rightarrow W + H + \nu$ [7]. As we can see, the $\gamma\gamma$ intermediate state is a more efficient way of producing a Higgs boson with $M_H \gtrsim 140$ GeV. It can lead to more than 100 Higgs events per year for a Higgs mass up to 320–400 GeV depending on the top quark mass, assuming a integrated luminosity $\mathcal{L}_{e^+e^-} = 100 \text{ fb}^{-1}$.

The cross section for a specific Higgs decay channel is obtained in the narrow width approximation by the product of the production cross section [Eq. (4)] and the corresponding decay branching ratio, which can be found elsewhere [2]. In Fig. 1(b) we show the cross section for the processes $e + \gamma \rightarrow e\gamma\gamma \rightarrow e + H \rightarrow e b \bar{b} (VV^*)$, with $V = W^\pm, Z$. The Higgs boson signal is dominated by different channels depending on its mass, and therefore the possibility of detecting the Higgs boson strongly depends on the mass value.

The most promising signal over background ratio is attained when the Higgs boson decays into the ZZ channel, which is important for $M_H \gtrsim 180$ GeV. Unlike in the $\gamma\gamma$ mode of the collider [4], where this channel is free of ir-

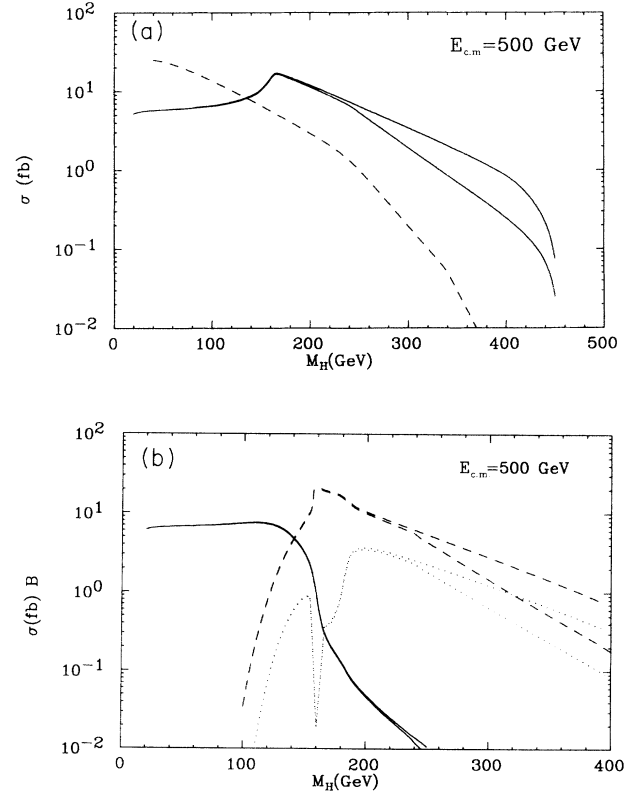


FIG. 1. (a) Total cross section at $\sqrt{s} = 500$ GeV for the process $e + \gamma \rightarrow e\gamma\gamma \rightarrow e + H$ (solid lines) and for the process $e + \gamma \rightarrow W + H + \nu$ (dashed line) versus the Higgs boson mass. The lower (upper) curve corresponds to $m_t = 120$ (200) GeV. (b) Total cross section at $\sqrt{s} = 500$ GeV for the process $e + \gamma \rightarrow e + H \rightarrow e b \bar{b}$ for different final states: $b\bar{b}$ (solid line), W^+W^- (dashed line), and ZZ (dotted line) as a function of the Higgs boson mass. For each type of line the lower (upper) curve corresponds to $m_t = 120$ (200) GeV.

reducible background at the tree level, in the $e\gamma$ mode there is a possible source of background via the process $e + \gamma \rightarrow e + Z + Z$, with the final electron going in the beam pipe. Moreover, it has been recently shown [10] that one-loop corrections generate an important contribution to the cross section $\gamma\gamma \rightarrow ZZ$ for large ZZ invariant masses giving rise to another source of background.

In Fig. 2 we compare the total cross section of the Higgs signal measured in fb with the invariant mass distribution (measured in fb/10 GeV) of the backgrounds [11]. In the computation of the background $e + \gamma \rightarrow e + Z + Z$ we assumed an angular size for the beam pipe of $\theta_e < 5^\circ$. The one-loop background has been computed for $m_t = 120$ GeV but it is very insensitive to the value of the top quark mass [10]. From Fig. 2(a) we see that for 500 GeV machine, assuming an invariant mass resolution of the order of 20 GeV, the Higgs signal overcomes the background in almost all the M_H range, without need of any further cut. Even though the one-loop background becomes more important at higher center-of-mass energies, the signal is still larger than the background in the M_H range we are considering, as illustrated in Fig. 2(b).

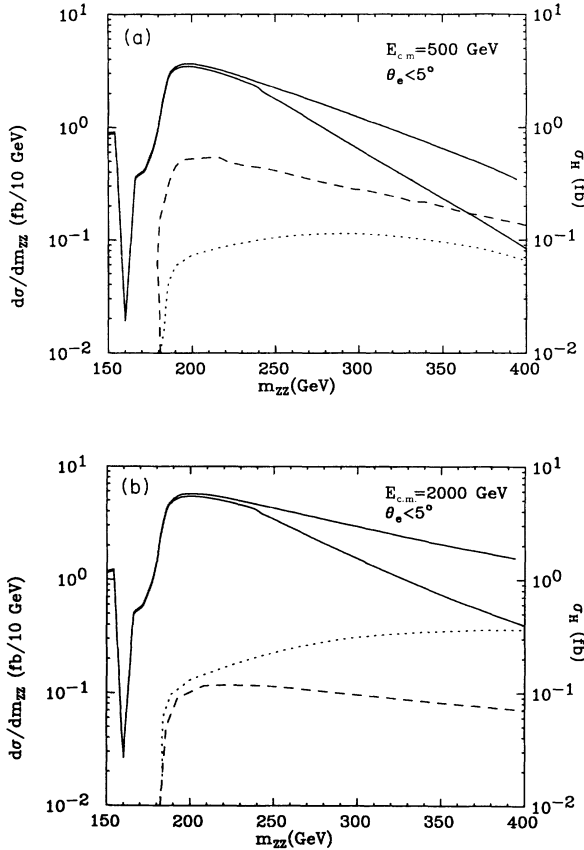


FIG. 2. (a) Total cross section for the Higgs signal $H \rightarrow Z^*Z$ measured in fb (solid line) and invariant mass distributions (measured in fb/10 GeV) of the $e + \gamma \rightarrow e + Z + Z$ background (dashed line) and one-loop $\gamma\gamma \rightarrow ZZ$ background (dotted line) for $\sqrt{s} = 500$ GeV. For the background we assume an angular size for the beam pipe of $\theta_e < 5^\circ$. The lower (upper) curves correspond to $m_t = 120$ (200) GeV. (b) Same as (a) for $\sqrt{s} = 2000$ GeV.

In the case of the W^+W^- channel the situation becomes worse. The background from $e + \gamma \rightarrow e + W^+ + W^-$ is large since it receives the main contribution from the effective photon process $e + \gamma \rightarrow e\gamma\gamma \rightarrow e + W^+ + W^-$, where, as in the Higgs signal, the electron escapes undetected. Since in the $\gamma\gamma$ center-of-mass frame the signal is isotropic while the background is forward-backward peaked [4], it is possible to improve the signal to background ratio by imposing a cut on the W scattering angle in that system. We chose $|\cos\theta_W| < 0.85$. As seen in Fig. 3 the background is still 1 order of magnitude larger than the signal. Assuming an invariant mass resolution of 20 GeV and an integrated luminosity of 100 pb^{-1} the signal has a significance of 3σ or more only for $M_H \lesssim 270$ GeV. Although this significance level allows us the detection of the Higgs boson in this mode, it makes the observation of the Higgs properties in this channel a hard task.

For a lighter Higgs boson, $M_H < 150$ GeV, we should rely on the $b\bar{b}$ decay channel. In this case there are large backgrounds coming from the direct photon process, $\gamma + \gamma \rightarrow b + \bar{b}$, and also from the once resolved photon ones, $\gamma + \gamma(g) \rightarrow b + \bar{b}$ [5], where the photon interacts via its gluonic content. Moreover, there are

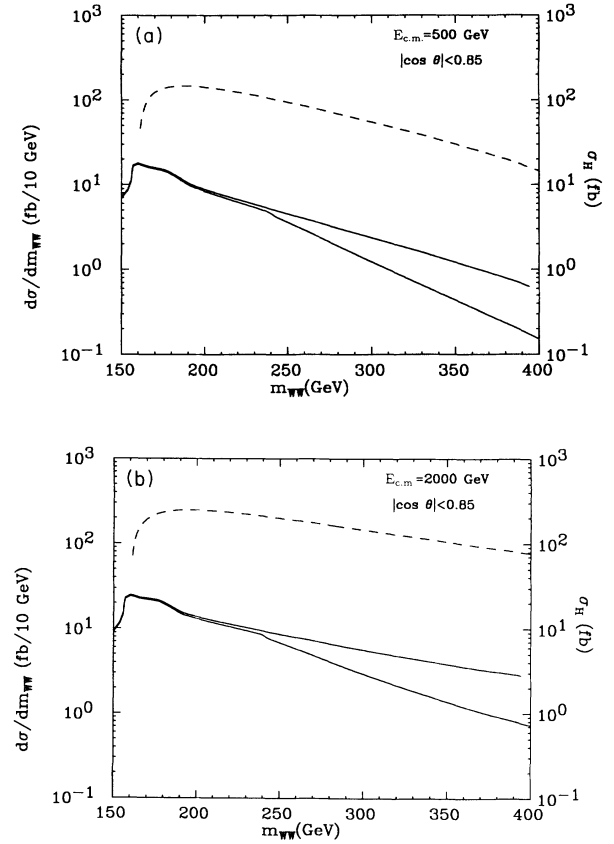


FIG. 3. (a) Total cross section for the Higgs signal $H \rightarrow W^*W$ measured in fb for $m_t = 120$ (lower solid line) and 200 GeV (upper solid line) and invariant mass distributions (measured in fb/10 GeV) of the background (dashed line) for $\sqrt{s} = 500$ GeV. We imposed the cut $|\cos\theta_W| < 0.85$. (b) Same as (a) for $\sqrt{s} = 2000$ GeV.

also large reducible backgrounds due to the production of charmed quarks, which can fake b quarks as they possess a production cross section which exceeds the b -pair background by up to 1 order of magnitude. Again we use the S -wave nature of the Higgs resonance to improve the signal to background ratio by requiring that the scattering angle of the b 's (c 's) with respect to the beam axis is large enough $|\cos\theta| < 0.85$ in the $b\bar{b}$ rest frame. Imposing this cut in all the following, we compare in Fig. 4(a) the total cross section of the Higgs signal $H \rightarrow b\bar{b}$, measured in fb, with the invariant mass distributions (measured in fb/10 GeV) of the various backgrounds. We used for illustration the parametrization by Drees and Grassie [12] (DG) which provides a relatively soft gluon distribution. Harder (softer) distributions such as the Levy-Abramowicz-Charchula set 3 (LAC3) [(LAC1)] parametrization of Ref. [13] would lead to larger [smaller] resolved backgrounds.

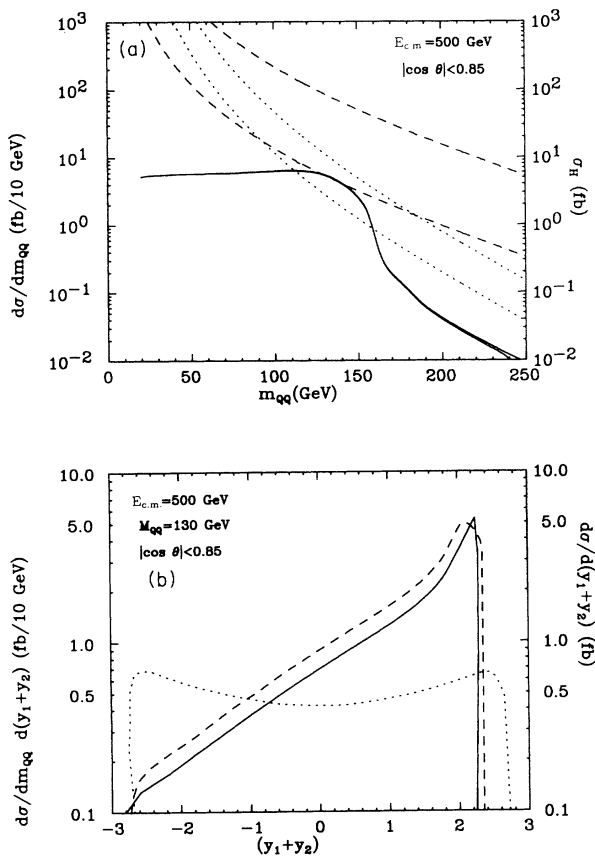


FIG. 4. (a) Total cross section for the Higgs signal $H \rightarrow b\bar{b}$ measured in fb (solid line) and invariant mass distributions (measured in fb/10 GeV) of the various backgrounds for $\sqrt{s} = 500$ GeV. The dashed lines correspond to the direct photon backgrounds. Dotted lines correspond to resolved photon backgrounds for DG photon structure functions. In all cases the lower (upper) line correspond to $b\bar{b}$ ($c\bar{c}$) background. We imposed the cut $|\cos\theta_Q| < 0.85$. (b) $(y_1 + y_2)$ distribution in the laboratory frame for the $b\bar{b}$ pairs. The Higgs signal and the different backgrounds are shown for the invariant mass of 130 GeV for the $b\bar{b}$ pair, using the same cuts and notation as in (a).

Figure 4(b) shows the $(y_1 + y_2)$ distribution in the laboratory frame for the quarks from signal and different backgrounds. In our convention, positive rapidity corresponds to the direction of the incoming backscattered photon. Both signal and direct backgrounds populate the positive rapidity region. Since the laser backscattered photons carry most of the electron beam energy while the bremsstrahlung process is dominated by soft photons, the jets tend to follow the initial backscattered photon. Resolved backgrounds, however, present a flat distribution since they receive two contributions which are kinematically separated [14]: in resolved processes where the bremsstrahlung photon is probed, the jets follow the initial backscattered photon and populate the positive rapidity region, while in those where laser backscattered photon is resolved the jets follow the direction of the bremsstrahlung photon and have negative values of $(y_1 + y_2)$. As a consequence the resolved background can be reduced by a factor of 50% approximately by imposing that $(y_1 + y_2) > 0$. We should remark that this kind of kinematical cut would be worthless in $\gamma\gamma$ collisions when both photons come from the laser backscattering mechanism. In this latter case, both the signal and the resolved background are expected to have approximately the same behavior over all the rapidity range [5].

The final results for the $b\bar{b}$ channel are shown in Fig. 5, where an invariant mass resolution of 20 GeV is assumed for the backgrounds (for a discussion on this point see Ref. [5]). A 90% efficiency for both b identification and c rejection would lead to a 3–6 σ effect for the Higgs boson mass in the range $75 < M_H < 155$ GeV, assuming an integrated luminosity of 100 fb^{-1} for the NLC with $\sqrt{s} = 500$ GeV. In order to improve the significance level of the signal and its potential to study the coupling $H\gamma\gamma$, we can consider two possibilities: first we can reduce the direct background (and increase the signal) by polarizing both the laser backscattered photon and the electron [4]. Second, the hadronic calorimeter should be able to give

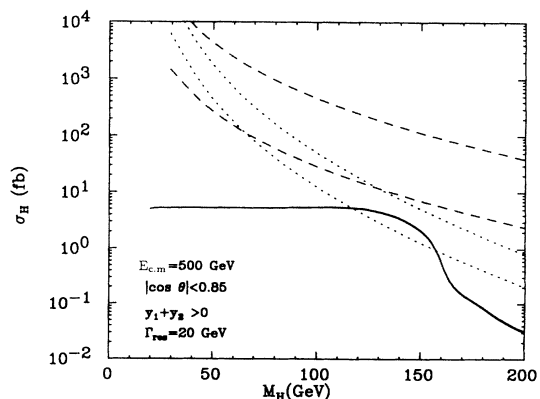


FIG. 5. Cross section for the Higgs signal and backgrounds (same notation as Fig. 4). For the backgrounds an invariant mass resolution $m_H \pm 10$ GeV is assumed. In all cases we require $|\cos\theta_Q| < 0.85$ in the $Q\bar{Q}$ rest frame and $|y_1 + y_2| > 0$ in the laboratory frame.

a good coverage close to the beam pipe in order to detect the jet associated with the remnants of the resolved photon, allowing one to veto the background coming from the gluonic content of the photon.

In conclusion, we demonstrate that the process $e + \gamma \rightarrow e\gamma\gamma \rightarrow e + H$ is able to yield a significant number of Higgs bosons in $e\gamma$ collisions. Furthermore, there is a large window where even the elusive intermediate-mass Higgs boson could be identified when we take into account the $\gamma\gamma$ fusion mechanism proposed in this paper. Through this mechanism we should also be able to measure the $H\gamma\gamma$ coupling, which can give us some hints about the Higgs boson coupling with all charged particles that acquire mass via the Higgs mechanism.

This work was supported by the University of Wisconsin Research Committee with funds granted by the Wisconsin Alumni Research Foundation, by the U.S. Department of Energy under Contract No. DE-AC02-76ER00881, by the Texas National Research Laboratory Commission under Grant No. RGFY9273, by Conselho Nacional de Desenvolvimento Científico e Tecnológico (CNPq-Brazil), and by the National Science Foundation under Contract No. INT 916182. M.C.G-G. is very grateful to Instituto de Física Teórica de Universidade Estadual Paulista and Instituto de Física de Universidade de São Paulo for their kind hospitality. We also want to thank M. Berger for enlightening conversations on the one-loop ZZ background.

-
- [1] F. R. Arutyunian and V. A. Tumanian, *Phys. Lett.* **4**, 176 (1963); R. H. Milburn, *Phys. Rev. Lett.* **10**, 75 (1963).
- [2] J. F. Gunion, H. E. Haber, G. Kane, and S. Dawson, *The Higgs Hunter's Guide* (Addison-Wesley, New York, 1990).
- [3] V. Barger, T. Han, and A. Stange, *Phys. Rev. D* **42**, 777 (1990).
- [4] J. F. Gunion and H. E. Haber, *Phys. Rev. D* **48**, 5109 (1993).
- [5] O. J. P. Éboli, M. C. Gonzalez-Garcia, F. Halzen, and D. Zeppenfeld, *Phys. Rev. D* **48**, 1430 (1993).
- [6] E. Boos *et al.*, *Z. Phys. C* **56**, 487 (1992).
- [7] E. Boos *et al.*, *Phys. Lett. B* **273**, 173 (1991); K. Hagiwara, I. Watanabe, and P. M. Zerwas, *ibid.* **278**, 187 (1992).
- [8] A detailed study of the reaction $e + \gamma \rightarrow W^- + H + \nu$ can be found in K. Cheung, *Phys. Rev. D* **48**, 1035 (1993).
- [9] I. F. Ginzburg, G. L. Kotkin, V. G. Serbo, and V. I. Telnov, *Nucl. Instrum. Methods* **205**, 47 (1983); **219**, 5 (1984); V. I. Telnov, *ibid. A* **294**, 72 (1990).
- [10] G. V. Jikia, *Phys. Lett. B* **298**, 224 (1993); M. Berger, *Phys. Rev. D* **48**, 5721 (1993).
- [11] The cross sections for the processes $e + \gamma \rightarrow V + V + e$, with $V = W$ or Z were obtained through the numerical evaluation of the amplitudes using a method similar to the one described in Ref. [3]. This cross section was also evaluated by K. Cheung, *Nucl. Phys.* **B403**, 572 (1993).
- [12] M. Drees and K. Grassie, *Z. Phys. C* **28**, 451 (1985).
- [13] H. Abramowicz, K. Charchula, and A. Levy, *Phys. Lett. B* **269**, 458 (1991).
- [14] O. J. P. Éboli, M. C. González-García, F. Halzen, and S. F. Novaes, *Phys. Lett. B* **301**, 115 (1993).